

**Higgs self-coupling as a probe of the electroweak phase transition**Andrew Noble<sup>\*</sup> and Maxim Perelstein<sup>+</sup>*Institute for High Energy Phenomenology, Newman Laboratory of Elementary Particle Physics, Cornell University,  
Ithaca, New York 14853, USA*

(Received 11 June 2008; published 11 September 2008)

We argue that, within a broad class of extensions of the standard model, there is a tight correlation between the dynamics of the electroweak phase transition and the cubic self-coupling of the Higgs boson: Models which exhibit a strong first-order electroweak phase transition predict a large deviation of the Higgs self-coupling from the standard model prediction, as long as no accidental cancellations occur. Order-one deviations are typical. This shift would be observable at the Large Hadron Collider if the proposed luminosity or energy upgrades are realized, as well as at a future electron-positron collider such as the proposed International Linear Collider. These measurements would provide a laboratory test of the dynamics of the electroweak phase transition.

DOI: [10.1103/PhysRevD.78.063518](https://doi.org/10.1103/PhysRevD.78.063518)

PACS numbers: 98.80.Cq

**I. INTRODUCTION**

About  $10^{-10}$  sec after the big bang, the Universe underwent a phase transition in which the electroweak gauge symmetry was reduced from  $SU(2)_L \times U(1)_Y$  to  $U(1)_{em}$ . In the standard model (SM) and many of its extensions, the electroweak phase transition (EWPT) is understood in terms of the dynamics of a fundamental scalar field, the Higgs  $h$ : the vacuum  $h = 0$  preferred at high temperatures becomes unstable at a certain “critical temperature”  $T_c$  and the Higgs field develops a vacuum expectation value (vev) [1]. The nature of this transition is a subject of considerable interest. For example, is the EWPT a violent, out-of-equilibrium event accompanied by massive entropy production (first-order transition) or a gentle, quasiadiabatic process (second-order transition)? Answering this question would have far-ranging implications; for example, electroweak baryogenesis, which theoretically is arguably the most attractive of the mechanisms proposed to explain the observed matter-antimatter asymmetry, can only occur if the EWPT is strongly first order [2]. It is very difficult to obtain direct information on the EWPT from astrophysical observations, due to the long and complex history of the Universe since the transition. (Note, however, that gravitational waves produced in a first-order transition might be observable at LISA [3].) Luckily, the dynamics of the phase transition can be deduced theoretically, once the fundamental Lagrangian governing the physics at the electroweak scale is known. For example, it is well known that if there is no physics beyond the SM relevant at that scale, the transition is never first order for the Higgs boson mass obeying the current experimental lower bound, 114.4 GeV [4]. Of course, the gauge hierarchy problem and other arguments strongly suggest that

physics beyond the standard model (BSM) should appear at the electroweak scale, and the nature of the EWPT depends on the (as yet unknown) details of that physics. Observing all of the weak-scale BSM particles and measuring their masses and interactions (in particular with the Higgs boson) would provide sufficient information to determine the order of the transition. In practice, however, this will be a very difficult task for the upcoming Large Hadron Collider (LHC), and even for a more distant next-generation  $e^+e^-$  collider such as the proposed International Linear Collider (ILC), especially in models where some of the new states are gauge singlets. It would therefore be useful to identify simpler observables that are correlated with the order of the transition. In this paper, we propose that the value of the Higgs boson cubic self-coupling is one such observable. Specifically, we argue that models leading to a first-order phase transition predict a large (typically order-one) deviation of the Higgs cubic coupling from its SM value. We show that this is the case in three toy models, which capture three basic mechanisms for obtaining a first-order EWPT: loop-induced corrections to the Higgs effective potential, nonrenormalizable operators in the potential, and mixing between the weak-doublet Higgs and singlet scalars at the weak scale. The only exceptions to this statement that were observed in our analysis are due to accidental cancellations between large corrections to the Higgs cubic of different origins. Thus, while nonobservation of a large deviation of the Higgs cubic from the SM prediction would not completely rule out a first-order EWPT, it would make it very unlikely.

The correlation between a strong first-order EWPT and a large deviation of the Higgs self-coupling from the SM value was already noted, in the specific contexts of low-cutoff models [5] and the two-Higgs doublet model [6]. Here, we will argue that this correlation is in fact much more general and applies (with a small caveat requiring no accidental cancellations) in a very broad class of models.

<sup>\*</sup>anoble@physics.cornell.edu<sup>+</sup>maxim@lepp.cornell.edu

## II. RENORMALIZABLE MODELS WITH UNMIXED HIGGS FIELD

In this paper, we will not restrict ourselves to a specific extension of the SM. We will instead study a series of toy models, which capture the important features of realistic BSM theories exhibiting strong first-order EWPT. The toy models analyzed in this section satisfy two basic conditions. First, the only scalar field which changes its value during the EWPT is the neutral component  $h$  of the SM Higgs doublet  $H = (G^+, (h + iG^0)/\sqrt{2})$ . The “SM Higgs doublet” is defined as a field whose tree-level couplings to all SM states are given by the SM values, with no large corrections from new physics: For example, no significant tree-level mixing of  $h$  with gauge-singlet scalars is allowed. With this assumption, the finite-temperature effective potential  $V_{\text{eff}}(h, T)$  completely specifies the dynamics of the EWPT. Second, at tree level, the Higgs sector is weakly coupled and can be adequately described by a renormalizable Lagrangian, i.e. no irrelevant terms are important. Many theoretically motivated models satisfy these conditions, including the minimal supersymmetric standard model (MSSM) [7] for a broad range of parameters corresponding to the so-called Higgs decoupling region, little Higgs models [8] such as the littlest Higgs with T-parity, and others. Interesting models which violate either one of these conditions and exhibit first-order EWPT also exist; we will study such examples in Secs. III and IV.

With the above conditions, the tree-level Higgs potential has the form

$$V'(h) = -\frac{\mu^2}{2}h^2 + \frac{\lambda}{4}h^4, \quad (1)$$

while the masses of the SM and BSM particles are given by

$$M_{0i}^2(h) = M_{0i}^2 + a_i h^2. \quad (2)$$

At the one-loop level, the Higgs effective potential, including finite-temperature corrections, can be determined completely once the values of  $M_{0i}^2$  and  $a_i$  for every particle in the theory are known. In practice, particles with  $a_i \ll 1$  (weak coupling to the Higgs) can be neglected. In the SM, these parameters are given by

$$i = (t, W, Z, h, G), \quad M_0^2 = (0, 0, 0, -\mu^2, -\mu^2), \quad (3)$$

$$a = \left( \frac{\lambda_t^2}{2}, \frac{g^2}{4}, \frac{g^2 + g'^2}{4}, 3\lambda, \lambda \right).$$

The zero-temperature (Coleman-Weinberg) correction to the potential (1), in the  $\overline{\text{MS}}$  regularization scheme, has the form

$$V_0^l(h) = \sum_i \frac{g_i(-1)^{F_i}}{64\pi^2} M_i^4 \left( \log \frac{M_i^2}{\Lambda^2} + C_i \right), \quad (4)$$

where  $\Lambda$  is the renormalization scale and  $g_i$  and  $F_i$  are the multiplicity and fermion number of the field  $i$ . In the SM,

in the basis of Eq. (3),  $g = (12, 6, 3, 1, 3)$  and  $F = (-1, 1, 1, 1, 1)$ . The constants  $C_i$  are regularization scheme dependent and are physically irrelevant, since their only effect is an additive renormalization of the parameters  $\mu^2$  and  $\lambda$  and the cosmological constant. Rescaling  $\Lambda$  has the same effect; we fix  $\Lambda = 174$  GeV and interpret  $\mu^2$  and  $\lambda$  as the values of the couplings at that scale. The parameters are subject to the constraint

$$\frac{d}{dh}(V'(h = v) + V_0^l(h = v)) = 0, \quad (5)$$

where  $v = 246$  GeV. In addition, the Higgs mass,

$$m_h^2 = \frac{d^2}{dh^2}(V'(h = v) + V_0^l(h = v)), \quad (6)$$

must satisfy the experimental lower bound,

$$m_h > 114.4 \text{ GeV}. \quad (7)$$

The potential defined in this way suffers from an infrared singularity that appears at the minimum of the tree-level potential,  $v_{\text{tree}}^2 = \mu^2/\lambda$ , and is due to the massless (Goldstone) bosons  $G$  at that point [9]. While the potential itself remains finite ( $\lim_{x \rightarrow 0} x^4 \log x^2 = 0$ ), the cubic coupling, defined as

$$\lambda_3 \equiv \frac{1}{6} \frac{d^3(V'(h) + V_0^l(h))}{dh^3} \Big|_{h=v}, \quad (8)$$

diverges at that point. Resummation of the infrared logarithms is required to correctly evaluate  $\lambda_3$  in the neighborhood of that point. This resummation is conveniently achieved by switching from the zero-momentum renormalization scheme to the on-shell scheme [9]. Technically, this is equivalent to adding an extra term to  $V_0^l$  and interpreting the second derivative at the minimum of the corrected potential as the physical (on-shell) Higgs mass. The additional term eliminates the infrared divergence. We will employ the on-shell scheme throughout this paper.

The one-loop finite-temperature potential has the form [10]

$$V_T(h, T) = \sum_{F_i=0} \frac{g_i T}{2\pi^2} \int dk k^2 \log[1 - \exp(-\beta\sqrt{k^2 + M_i^2(h)})] - \sum_{F_i=1} \frac{g_i T}{2\pi^2} \int dk k^2 \log[1 + \exp(-\beta\sqrt{k^2 + M_i^2(h)})], \quad (9)$$

where  $\beta = 1/T$ . If the model contains bosons with masses small compared to  $T$ , multiloop infrared-divergent contributions need to be included to correctly analyze the dynamics of  $h$ . These contributions can be resummed and written in the form of the “ring potential” [11]:

$$V_r(h, T) = \sum_i \frac{T}{12\pi} \text{Tr}[M_i^3(h) - (M_i^2(h) + \Pi_i(0))^{3/2}], \quad (10)$$

where the sum runs over all (light) bosonic degrees of freedom, and  $\Pi_i(0)$  is the zero-momentum polarization tensor. In the SM,

$$\begin{aligned} \Pi_h(0) &= \Pi_G(0) = T^2 \left( \frac{3}{16} g^2 + \frac{1}{16} g'^2 + \frac{1}{4} \lambda_t^2 + \frac{1}{2} \lambda \right), \\ \Pi_{GB}(0) &= \frac{11}{6} T^2 \text{diag}(g^2, g^2, g'^2, g'^2), \end{aligned} \quad (11)$$

and

$$M_{GB}^2(h) = \frac{h^2}{4} \begin{pmatrix} g^2 & 0 & 0 & 0 \\ 0 & g^2 & 0 & 0 \\ 0 & 0 & g'^2 & -gg'^2 \\ 0 & 0 & -gg'^2 & g'^2 \end{pmatrix}. \quad (12)$$

These expressions are valid at  $T \gg M_W$ ; for smaller  $T$ , the ring terms are unimportant and can be dropped. The full potential is  $V_{\text{eff}}(h; T) = V^l + V_0^l + V_T + V_r$ . A useful “decoupling” feature of this potential is that at any  $T$ , the contributions from particles with  $M_i(h) \gg T$  are exponentially suppressed. Thus, in BSM theories, only weak-scale states need to be included to analyze the EWPT. For some values of  $h$ , the potential  $V(h, T)$  develops an imaginary part, due to the quantum instability of a classical state with a spatially uniform value of  $h$  [12]. This effect does not affect the dynamics of a first-order transition, as long as the rate of this instability is small compared to the electroweak scale. This condition is always satisfied in our analysis.

At high temperature,  $T \gg M_{0i}$  for all states, the potential has the simple form

$$V_{\text{eff}}(h; T) \approx \left( \sum_{F_i=0} g_i a_i + \frac{1}{2} \sum_{F_i=1} g_i a_i \right) \frac{T^2 h^2}{24}. \quad (13)$$

If the quantity in brackets is positive,  $\langle h \rangle = 0$  is a stable minimum, and the electroweak symmetry is restored. This is the case, for example, in the SM and the MSSM, where  $a_i > 0$  for all states. We will restrict our analysis to such models, since otherwise the EWPT does not occur. A first-order transition occurs if  $V_{\text{eff}}(h; T)$  develops a second, symmetry-breaking local minimum,  $\langle h \rangle \equiv v_T(T) \neq 0$ , while the high-temperature minimum  $\langle h \rangle = 0$  is still classically stable. Then, once the symmetry-breaking vacuum becomes energetically preferred, bubbles of the symmetry-breaking vacuum will start rapidly nucleating, growing, and coalescing, eventually encompassing the entire Universe and completing the phase transition. The critical temperature  $T_c$  at which the phase transition occurs can be

found from the condition<sup>1</sup>

$$V_{\text{eff}}(\langle h \rangle = 0; T_c) = V_{\text{eff}}(v_T(T_c); T_c). \quad (14)$$

The “strength” of the first-order transition (more precisely, the degree of deviation from quasiadiabatic evolution) can be characterized by the dimensionless parameter

$$\xi = \frac{v_T(T_c)}{T_c}. \quad (15)$$

For example, it is well known that successful electroweak baryogenesis requires  $\xi \gtrsim 1$ .

Because of the complicated form of the potential, the problem of finding  $T_c$  and  $v_T(T_c)$  in a given model is in general not tractable analytically. We have developed a numerical code which is used to evaluate these quantities in all examples studied in this paper.

In the SM, the EWPT is always second order once the bound (7) is satisfied. Below, we analyze the situation in a few simple extensions of the SM.

### A. Single BSM scalar

Consider a toy model in which a single real scalar state is added to the SM, with the potential

$$V = \frac{1}{2} M_0^2 S^2 + \zeta^2 |H|^2 S^2. \quad (16)$$

This is the most general renormalizable potential which respects a symmetry  $S \rightarrow -S$ . (Without this symmetry, tree-level mixing between  $h$  and  $S$  would generally occur. Such models will be discussed below.) Note that while we use the SUSY-inspired notation  $\zeta^2$  for the coefficient in Eq. (16), this coefficient can in general be negative, as long as  $S$  does not become tachyonic until  $h > v$  and the lifetime of the vacuum at  $(h = v, S = 0)$  is larger than the present age of the Universe. (The runaway direction can be stabilized by the addition of a small  $S^4$  term, which does not affect our analysis.) We include the models with negative values of  $\zeta^2$  in the analysis in order to demonstrate that they exhibit the same correlation between the Higgs cubic coupling and the  $\xi$  parameter as the positive- $\zeta^2$  models. We imposed the constraint that  $S$  should not be tachyonic in the range  $h = 0 \dots 300$  GeV, but did not analyze the lifetime of the conventional electroweak symmetry-breaking (EWSB) vacuum for these models, so some of the negative- $\zeta^2$  points may be phenomenologically unacceptable. A detailed analysis of this issue is beyond the scope of this paper, and its outcome would not affect the main point of our argument in any way.

<sup>1</sup>Note that the actual transition temperature may be lower if the bubble nucleation rate  $\Gamma$  is strongly suppressed compared to its natural value,  $\Gamma \sim v$ . Phase transition does not occur until  $\Gamma \sim H \sim v^2/M_{\text{Pl}}$ . Given the large hierarchy  $v \ll M_{\text{Pl}}$ , we will not include this possibility in our analysis.

The scalar contribution to the one-loop effective potential is given by Eqs. (4), (9), and (10), where  $M(S) = M_0^2 + \zeta^2 h^2$ ,  $\Pi_S(0) = \frac{1}{3} T^2 \zeta^2$ , and  $g_S = 1$ . In addition, the ring terms due to the  $h$  and  $G$  fields have to be modified by adding the scalar contribution to the polarization tensors,  $\Delta\Pi_h(0) = \Delta\Pi_G(0) = \frac{1}{12} T^2 \zeta^2$ . (We neglect additional contributions to polarization tensors due to  $S$  self-coupling or coupling to other BSM singlets.) In order to identify the points with a first-order EWPT, we scanned the parameters of the model:  $M_0 = 0 \dots 800$  GeV,  $\zeta^2 = -4 \dots 8$ . We also scanned the parameters  $\mu$  and  $\lambda$ , making sure that the constraints (5) and (7) are satisfied; the scanned region corresponds to  $m_h = 114.4 \dots 244.4$  GeV. (We did not find any points with higher  $m_h$  and a strong first-order EWPT.) For every point exhibiting a first-order EWPT, we compute the one-loop value of the physical Higgs boson cubic self-coupling, using Eq. (8). The results are presented in Fig. 1. In the left panel, we plot the parameters  $\xi$  and  $\lambda_3$  (normalized to the SM one-loop value) for the points in our scan; in the right panel, we plot  $m_h$  and  $\lambda_3$ . It is clear from the plots that the Higgs self-coupling is significantly larger than the SM value for *all* points with a first-order EWPT in this model. If  $m_h$  is known from experiment (as it surely will be, by the time the experiments become sensitive to the Higgs self-coupling), the correlation between  $\lambda_3$  and  $\xi$  becomes tighter, as illustrated in Fig. 2.

Experimental measurement of  $\lambda_3$  requires collecting a significant sample of events with two Higgs bosons in the final state. At the LHC, this coupling can be determined with 20%–30% precision for the Higgs mass between 160 and 180 GeV, for integrated luminosity of 3000 fb<sup>-1</sup>, which can be achieved if the luminosity upgrade to 10<sup>35</sup> cm<sup>-2</sup> s<sup>-1</sup> is realized [13]. If an energy upgrade to a 200 TeV VLHC (very large hadron collider) is realized, the coupling can be measured with 8%–25% precision for

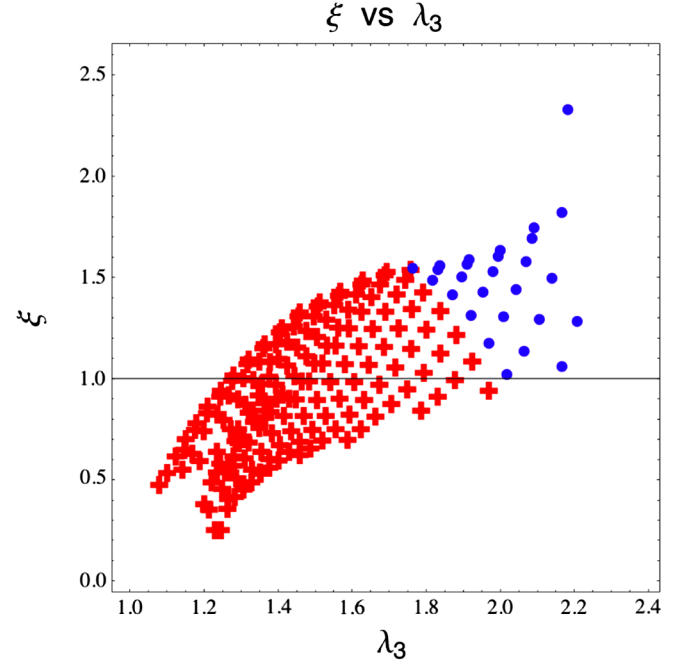


FIG. 2 (color online). Same as left panel of Fig. 1, but with the Higgs mass fixed at 160 GeV.

150 GeV <  $m_h$  < 200 GeV [14]. For lower Higgs masses, the VLHC could make a similarly precise measurement of  $\lambda_3$  using rare decays [15]. Also, the 500-GeV ILC is expected to measure  $\lambda_3$  with 20% accuracy for  $m_h$  < 140 GeV and a luminosity of 1 ab<sup>-1</sup> [16,17]. Our analysis shows that if a strong first-order EWPT occurs due to an extra scalar contribution at one loop, and the Higgs is sufficiently light, these experiments will discover a deviation of  $\lambda_3$  from the SM prediction. Higher center-of-mass energy would be required if  $m_h$  is larger; note, however, that strong first-order EWPT in this setup requires  $m_h \lesssim$

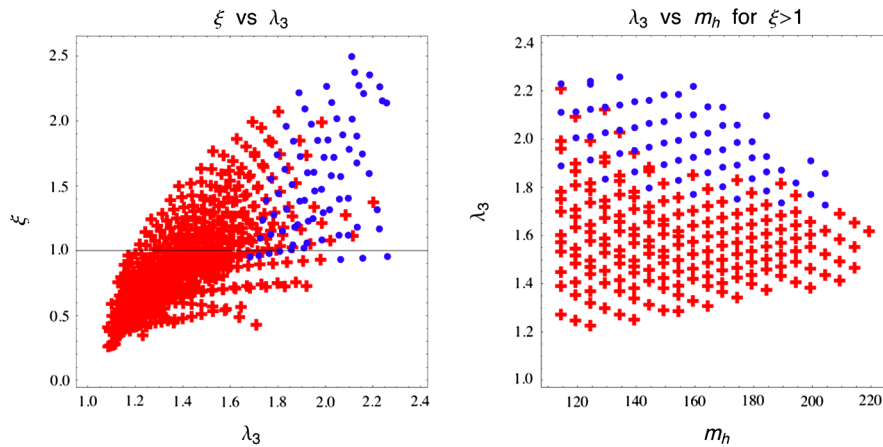


FIG. 1 (color online). SM with a single extra scalar. Models with a “bumpy” zero-temperature Higgs potential are shown by (blue) circles, and those without the bump by (red) crosses. Left panel: the strength of the first-order EWPT  $\xi$ , defined in Eq. (15), vs Higgs cubic self-coupling. Right panel: Higgs cubic self-coupling vs Higgs mass for points exhibiting a strong first-order EWPT,  $\xi > 1$ . In both plots, the Higgs self-coupling is normalized to the one-loop SM expectation for the same  $m_h$ .



250 GeV, so a modest increase in  $\sqrt{s}$  would be sufficient to cover all of the interesting parameter space.

In order to better understand this result, consider our model with  $\mu = M_0 = 0$ . In this case, the one-loop Higgs potential at zero temperature has the form

$$V_0 \approx \frac{1}{4} \lambda h^4 + \frac{A}{64\pi^2} h^4 \log \frac{h^2}{\Lambda^2}, \quad (17)$$

where  $A$  can be expressed in terms of the coupling constants of the model, and the contributions from Higgs loops have been neglected. If  $A > 0$  (which occurs for sufficiently large  $\zeta^2$  in our model), this potential has a stable symmetry-breaking minimum at  $h = \Lambda \exp(-8\pi^2 \lambda/A - 1/4)$  and a shallow local maximum at  $h = 0$ . This is of course just a realization of the purely radiative EWSB via dimensional transmutation (DT) *à la* Coleman and Weinberg [18]. If now a small *positive* Higgs mass term  $\mu^2 > 0$  is added, the potential around  $\phi = 0$  is dominated by this mass term, and the maximum at the origin is turned into a minimum. At the same time, if  $\mu^2$  is sufficiently small, the symmetry-breaking minimum is preserved, resulting in a potential with a “bump” between the two minima. A bumpy zero-temperature potential essentially guarantees that the EWPT will be of the first order, and most of the points with strong first-order EWPT in our scan (the blue points in Fig. 1) have this feature. The Higgs self-coupling for the pure DT potential, Eq. (17), is 66% larger than the (tree-level) SM value<sup>2</sup> for the same  $v$  and  $m_h$ :

$$\lambda_3^{\text{DT}} = \frac{5m_h^2}{6v} = \frac{5}{3} \lambda_3^{\text{SM, tree}}, \quad (18)$$

which is roughly at the center of the range for the models with strong first-order EWPT in our scan. Even without the bump (red points in Fig. 1), the models with  $\xi \geq 1$  have zero- $T$  potentials whose characteristic feature is a flatter maximum at  $h = 0$  compared to the SM. This shape is close to the DT potential, again resulting in large deviations of  $\lambda_3$  from the SM prediction.

The connection with the pure DT case points to a potential concern about our model: In the DT case, the physical Higgs mass is given by  $m_h = A^{1/2} v/(4\pi)$ , so that large values of  $A$  are required to satisfy the experimental lower bound on  $m_h$ . Correspondingly, in our scans, fairly large values of  $\zeta^2$  (between 3 and 10) are required to obtain phenomenologically consistent points with a strong first-order EWPT. For  $\zeta^2 \sim 10$ , one might worry about the validity of perturbation theory that was used in our analysis. Even for more moderate  $\zeta^2 = 3 \dots 5$ , two-loop corrections might be numerically significant. This is the case, for example, in the MSSM, where the stops effectively contribute with  $\zeta_{\text{eff}}^2 = \sqrt{12} \lambda_t^2 \approx 3.5$  (see Sec. IID). On the

other hand, the main outcome of our analysis is not the precise values of  $\lambda_3$  for each point in the scan, but the fact that the deviation from the SM in this quantity is large for models with strong first-order EWPT. It seems very unlikely that the higher-loop corrections would conspire to cancel the large one-loop correction to  $\lambda_3$  and bring it back precisely to the SM value, so our main qualitative conclusion should continue to hold even at strong coupling.

It should be noted that it is possible to have a large deviation of  $\lambda_3$  from the SM prediction *without* a strong first-order transition. We found such points in our scan. These points have values of  $m_0$  above, but not too far from, the Higgs vev  $v$ , and large values of  $a$ . The zero-temperature effective potential receives a correction of order  $a(v/m_0)^2$ , giving a substantial correction to  $\lambda_3$ ; the correction to the finite-temperature potential decouples exponentially, as  $\exp(-m_0/T)$ , and is not sufficient to yield a first-order transition. Thus, while an observation of a large correction to  $\lambda_3$  would keep the door open to the possibility of a strong first-order phase transition scenario, it would not prove it.

## B. Single BSM fermion

Consider the SM with a single additional Weyl fermion  $\chi$ , with a Majorana mass term

$$\left( M_0 + \frac{H^\dagger H}{\Lambda} + \dots \right) \chi \chi, \quad (19)$$

where dots denote higher-order nonrenormalizable terms. The mass has the form (2) with  $a = M_0/\Lambda$ , and the formalism presented above applies, with  $g_\chi = 2$ . Adding a single fermion also modifies the ring contributions:  $\Delta \Pi_h(0) = \Delta \Pi_G(0) = \frac{g}{24} T^2 a$ , where  $a$  is the same coefficient appearing in Eq. (2), and  $g = 2(4)$  for a Weyl (Dirac) fermion. We neglect additional ring contributions that would arise if  $\chi$  coupled to other BSM states. In this model, we performed the scan with  $m_h = 114.4 \dots 414.4$  GeV,  $M_0 = 0 \dots 800$  GeV, and  $a = -4 \dots 8$ . For  $a > 0$ ,  $\lambda_3$  is always suppressed with respect to the SM value, while for  $a < 0$ ,  $\lambda_3$  is enhanced. (In the  $T = 0$  effective potential, an  $a < 0$  fermion behaves like an  $a > 0$  boson, and vice versa.) But in neither case do we find a strong ( $\xi > 1$ ) first-order EWPT.

Since the only inputs from the model into the EWPT analysis are the coefficients in the mass formula (2), the same analysis applies in a model with a single Dirac BSM fermion (with  $M_0 = 0$  if the fermion is chiral, and possibly  $M_0 \neq 0$  if it is vectorlike). The only change is the new multiplicity factor,  $g_\Psi = 4$ . This does not affect the conclusions.

## C. A Single BSM scalar-fermion pair

Any realistic extension of the SM has multiple bosonic and fermionic states, whose contributions to the Higgs

<sup>2</sup>The same relation holds in any model with approximate conformal symmetry in the Higgs sector broken by nearly marginal operators [19].

effective potential must be added. In this subsection, we will explore how the interplay between bosonic and fermionic contributions affects the connection between the Higgs cubic coupling and the strength of a first-order EWPT. To address this, consider a toy model with a single fermion (for concreteness, we assume it to be a vectorlike Dirac fermion), and four identical scalars. The number of scalars is chosen so that the number of bosonic and fermionic degrees of freedom is the same, as would be the case in supersymmetric models. We searched for points with strong first-order EWPT in the following parameter space:  $a_s = a_\Psi = -1 \dots 4$ ,  $M_0^S = 0 \dots 600$  GeV,  $M_0^\Psi = 0 \dots 600$  GeV,  $m_h = 114.4 \dots 294.4$  GeV. (We did not find any points with a strong first-order EWPT for higher  $m_h$ .) The results are shown in Fig. 3. In most of the parameter space, the correlation between  $\xi$  and  $\lambda_3$ , observed above in the purely scalar model, persists, and models with strong first-order EWPT predict observable enhancements of  $\lambda_3$  with respect to the SM value. There is also a smaller region where an observable suppression of  $\lambda_3$  is predicted; this is due to the dominance of the fermion loops, which contribute to  $\lambda_3$  with a negative sign, for  $M_0^\Psi < M_0^S$ . There is also, however, an exceptional parameter region, in which  $\lambda_3$  is close to the SM value. This region has the following origin. In the one-loop zero-temperature potential, fermion and scalar contributions cancel if  $M_0^S = M_0^\Psi$  and  $a_s = a_\Psi$ , since  $S$  and  $\Psi$  form an exact supermultiplet, and  $\lambda_3$  has its SM value. The scalar and fermion contributions to the finite-temperature part of the potential, however, do not cancel in this limit. In particular, if  $a_s$  is large, a large cubic term can be generated at high temperature, which can lead to a first-order transition. Fermion loops do not contribute to this term. This explanation highlights the exceptional nature of the region with SM-like  $\lambda_3$ : the relations  $M_0^S = M_0^\Psi$  and  $a_s = a_\Psi$  cannot be enforced by a symmetry other than SUSY, which however

must be broken in the  $S - \Psi$  sector due to its strong coupling to the SM through the Higgs field. Thus, the cancellation should be regarded as accidental. In the absence of accidents, the  $\lambda_3 - \xi$  correlation works well in this model.

### D. Multiple BSM states

So far, we have observed the correlation between  $\lambda_3$  and  $\xi$  in simple toy models. Will it persist in realistic BSM theories with more complicated spectra and interactions? While it is clearly impossible to analyze all possible cases, it seems very likely that the answer is positive. Several arguments point in this direction.

First, note that in a model with  $N$  real (or  $N/2$  complex) scalar fields with identical masses and couplings, the zero-temperature potential  $V_{T=0}(h) = V' + V_0^I$  is exactly the same (up to terms of the two-loop order, not included in our approximation) as that for an “effective” single real scalar with rescaled couplings:

$$\begin{aligned} V_{T=0}(h; g = N; \lambda, \mu, M_0^2, \xi^2, \dots) \\ = V_{T=0}(h; g = 1; \lambda_{\text{eff}}, \mu_{\text{eff}}, M_{0,\text{eff}}^2, \xi_{\text{eff}}^2, \dots), \\ M_{0,\text{eff}}^2 = \sqrt{N} M_0^2, \quad \xi_{\text{eff}}^2 = \sqrt{N} \xi^2, \\ \lambda_{\text{eff}} = \lambda - \frac{N \xi^4 \log N}{32 \pi^2}, \\ \mu_{\text{eff}}^2 = \mu - \frac{N \xi^2 M_0^2 \log N}{32 \pi^2}, \end{aligned} \quad (20)$$

where the dots denote all other couplings and masses entering the potential, which do not need to be rescaled at this order. Inspecting Eqs. (9) and (10) shows that the same scaling applies for the scalar contribution to the finite-temperature potential (including rings), except one has to also rescale the temperature:

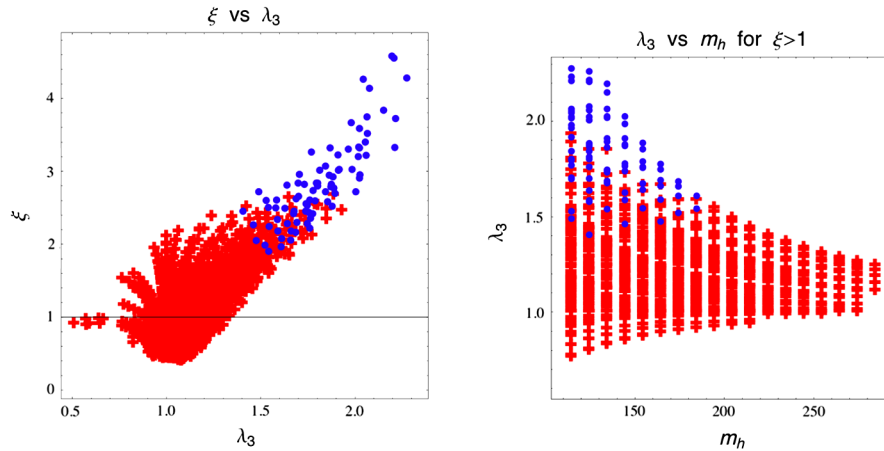


FIG. 3 (color online). SM with a single extra scalar-fermion pair. Models with a bumpy zero-temperature Higgs potential are shown by (blue) circles, and those without the bump by (red) crosses. Left panel: the strength of the first-order EWPT  $\xi$ , defined in Eq. (15), vs Higgs cubic self-coupling. Right panel: Higgs cubic self-coupling vs Higgs mass for points exhibiting a strong first-order EWPT,  $\xi > 1$ . In both plots, the Higgs self-coupling is normalized to the one-loop SM expectation for the same  $m_h$ .

$$V_T(h; g = N; T; M_0^2, \xi^2) = V_T(h; g = 1; N^{1/4}T; M_{0,\text{eff}}^2, \xi_{\text{eff}}^2). \quad (21)$$

If the scalar contribution dominates the thermal potential, this scaling approximately applies to the full thermal potential. We checked numerically that for points with first-order EWPT, the scaling is accurate to within 20%. The model with the  $N$  scalar field and its single-field counterpart have approximately the same potential at the critical temperature, and thus the same value of  $v_T(T_c)$ . The value of  $T_c$  in the effective single-field model is a factor of  $N^{1/4}$  higher than in the  $N$ -field model, so the  $\xi$  parameter in the single-field model is somewhat lower. The value of  $\lambda_3$  is the same in both models, since their zero-temperature potentials are identical. Thus, we expect the correlation between  $\xi$  and  $\lambda_3$  observed in the single-field case to persist in the  $N$ -field model. The minimal numerical value of the deviation of  $\lambda_3$  from the SM may be reduced somewhat in the  $N$ -field model compared to the single-field case, due to the scaling of  $\xi$ . However, since this scaling is mild,  $N^{1/4}$ , for moderate  $N$  we expect this effect to be small. (For large  $N$ , the perturbative one-loop analysis performed here is no longer applicable, and it is not clear how much reduction can be obtained by increasing  $N$ .) The same approximate scaling laws apply to models with  $N$  identical species of fermions as well. Since the gauge charges of the added states have no effect on the Higgs potential in the one-loop approximation, we conclude that the results of our toy-model analyses in fact apply, at least approximately, to *any* model where a single multiplet (or a single supermultiplet) dominates the BSM contribution to the Higgs potential, and this contribution can be analyzed within perturbation theory. The MSSM with light stops, and models with multiple gauge-singlet scalars as in Ref. [20], are in this category.

Even if multiple BSM states with different masses and couplings contribute to the Higgs potential, the qualitative picture should remain the same. In fact, we checked that a toy model with two scalars, whose masses and Higgs couplings are varied independently, produces results very similar to the single-scalar case. This is reasonable, since the similarity between the properties of the models with strong first-order EWPT and the DT model, noticed in Sec. II A, should persist independently of the precise origin of the large radiative corrections to the Higgs potential.

Based on this evidence, we believe that significant deviation of the Higgs cubic self-coupling from the SM value is a generic prediction of weakly coupled models of EWSB with strong first-order EWPT, provided that no accidental cancellations occur. A measurement of this coupling can serve as a diagnostic tool to glean information about the nature of the EWPT. This would be particularly valuable in models with extra gauge singlets, whose masses and couplings to the Higgs are difficult to measure directly, especially if the decay  $h \rightarrow SS$  is kinematically forbidden.

### III. A MODEL WITH NONRENORMALIZABLE HIGGS INTERACTIONS

The effect of new physics at the scale  $\Lambda \gg v$  on the Higgs potential can be parametrized by adding nonrenormalizable operators, suppressed by powers of  $\Lambda$ , to the potential. Grojean, Servant, and Wells (GSW) pointed out that in the presence of such terms, strong first-order EWPT may occur [5,21,22]. Following GSW, consider a model with a tree-level Higgs potential of the form

$$V(H) = \mu^2 H^\dagger H + \lambda (H^\dagger H)^2 + \frac{1}{\Lambda^2} (H^\dagger H)^3. \quad (22)$$

It is reasonable to use this effective theory to describe the EWPT if the electroweak symmetry-breaking vev is small compared to  $\Lambda$ . The strong first-order EWPT occurs for positive  $\mu^2$  and negative  $\lambda$ . With these choices, it can be shown that the theory is applicable only if  $|\lambda| \ll 1$ . In general, this requires fine-tuning; for example, if the dimension-6 operator arises due to exchanges of a heavy weak-singlet scalar, one can show that  $|\lambda| \sim 1$  will also be generated when the scalar is integrated out. This should be cancelled by a bare term in the Lagrangian. However, given the relatively low values of  $\Lambda$  interesting for our analysis (500 GeV–1 TeV range), the required fine-tuning is numerically quite modest. The appropriate suppression of the quartic coupling can occur naturally in composite Higgs models [23].

We analyzed the dynamics of the EWPT in the GSW model, following the general framework discussed in Sec. II. We performed a scan of the following parameters:  $m_h = 114.4 \dots 214.4$  GeV,  $\Lambda = 100 \dots 1000$  GeV. (We did not find any points with strong first-order EWPT for higher  $\Lambda$  and  $m_h$ .) Our results for the order of the transition are roughly consistent<sup>3</sup> with Refs. [5,22]. We also computed the Higgs cubic self-coupling (at the one-loop order) for each point in the scan. The results are shown in Fig. 4. In the region where there is a strong first-order EWPT, this model also predicts a large, order-one enhancement of  $\lambda_3$  from its SM value, which will be easily observable at the ILC. This is easy to understand analytically: at tree level, we have

$$\frac{\lambda_3^{\text{GSW}}}{\lambda_3^{\text{SM}}} = 1 + \frac{2v^4}{m_h^2 \Lambda^2}. \quad (23)$$

Since a strong first-order EWPT can only occur for  $\Lambda$  in the 500 GeV–1 TeV range, the correction term is large for

<sup>3</sup>Quantitative differences between our analysis and those of Refs. [5,22] arise due to different approximations made in each analysis. Our analysis includes the full SM contributions to  $V_0^l$ ,  $V_T$ , and  $V_r$ , listed in Sec. II, which were not included in Ref. [5]. On the other hand, we do not include the corrections to the one-loop potential and ring terms induced by the dimension-6 operator, and do not account for the possibility of delayed nucleation. Both effects were included in Ref. [22]. These differences do not affect the argument of this paper.

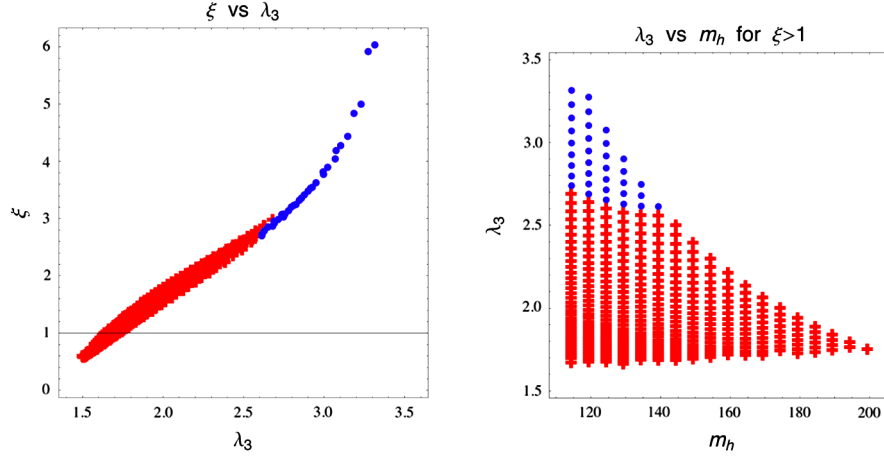


FIG. 4 (color online). SM with an  $H^6$  operator. Models with a bumpy zero-temperature Higgs potential are shown by (blue) circles, and those without the bump by (red) crosses. Left panel: the strength of the first-order EWPT  $\xi$ , defined in Eq. (15), vs Higgs cubic self-coupling. Right panel: Higgs cubic self-coupling vs Higgs mass for points exhibiting a strong first-order EWPT,  $\xi > 1$ . In both plots, the Higgs self-coupling is normalized to the one-loop SM expectation for the same  $m_h$ .

these points. [The one-loop corrections to Eq. (23) are at most about 10% in our scan.] In addition, as Fig. 4 indicates, there is a clear and strong correlation between this coupling and the strength of the EWPT.

#### IV. A MODEL WITH TREE-LEVEL HIGGS-SINGLET MIXING

In all examples studied above, the SM-like Higgs field  $h$  was the only field that acquired an expectation value during the EWPT. If other scalar fields are present, they may change their value in the same transition, so that the order parameter for the EWPT is effectively a linear combination of  $h$  and other fields. Of particular interest are models with extra gauge-singlet scalars, such as the NMSSM, certain little Higgs models, and others. At low temperatures, both singlet and Higgs vevs are generically nonzero. At high temperatures, the Higgs vev is driven to zero, and although the singlet vev typically remains nonzero, the EWPT involves changes in both vevs. Since the zero-temperature singlet potential is not restricted to even-degree polynomials by gauge invariance, it may contain cubic terms, which can naturally produce large “bumps” and lead to strong first-order EWPT. We will consider a simple model of this kind in this section. Our main goal here is to illustrate that the connection between the strong first-order EWPT and observable deviations of the Higgs self-coupling from the SM value persists in this model.

Many studies of models of this type have appeared in the literature, mostly in the context of the NMSSM and the nMSSM [24]. We will follow the conventions of a recent analysis by Profumo, Ramsey-Musolf, and Shaughnessy [25], which applies more generally. (See also Ref. [26].) Consider a model with a single real scalar  $S$  added to the SM. The most general renormalizable scalar potential has the form

$$V'(H, S) = -\mu^2 H^\dagger H + \lambda(H^\dagger H)^2 + \frac{a_1}{2} H^\dagger H S + \frac{a_2}{2} H^\dagger H S^2 + \frac{b_2}{2} S^2 + \frac{b_3}{3} S^3 + \frac{b_4}{4} S^4, \quad (24)$$

where  $H = (H^+, H^0)$ . We assume that the model has a stable vacuum at  $\langle H^0 \rangle = v/\sqrt{2}$ ,  $\langle S \rangle = s$ . (The conditions for this are listed in Ref. [25].) The physical Higgs fields are obtained by expanding around this minimum,  $H^0 = (h + v)/\sqrt{2}$  and  $S = s + x$ , and diagonalizing the mass matrix by a rotation

$$h_1 = \sin\theta s + \cos\theta h, \quad h_2 = \cos\theta s - \sin\theta h. \quad (25)$$

The mixing angle is defined such that  $|\cos\theta| > 1/\sqrt{2}$ . With this convention,  $h_1$  is more doubletlike and  $h_2$  is more singletlike. For positive (negative)  $\theta$ , the eigenmass  $m_2$  is greater than (less than)  $m_1$ .

We focus on the state  $h_1$ , which for simplicity we will refer to simply as “the Higgs,” and study the deviation of its cubic self-coupling from the SM prediction for a Higgs of the same mass. At tree level,

$$\frac{\lambda_3^{\text{PRS}}}{\lambda_3^{\text{SM}}} = \frac{v}{6m_1^2} (12v\lambda\cos^3\theta + 3a_1\cos^2\theta\sin\theta + 6a_2(x\cos\theta + v\sin\theta)\cos\theta\sin\theta + 4b_3\sin^3\theta + 12b_4x\sin^3\theta). \quad (26)$$

Unlike the models studied in Sec. II, no large couplings are required to achieve first-order EWPT in this setup. We restrict our analysis to the points where all couplings are weak, and ignore the loop corrections to the relation (26).

It is straightforward to compute the finite-temperature one-loop potential in this model and analyze the dynamics of the EWPT numerically. We used the high-temperature approximation for  $V'$ , expanding it up to linear order in  $T$ .



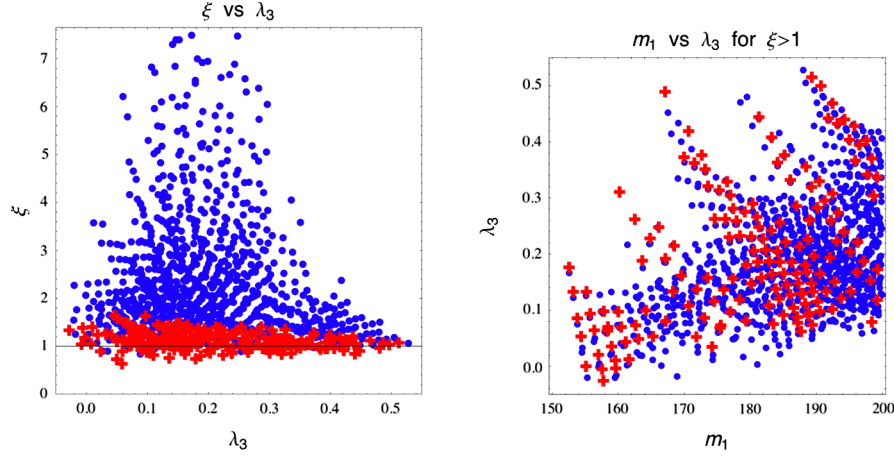


FIG. 5 (color online). SM with a single extra scalar that mixes with the Higgs. Models with a bumpy zero-temperature Higgs potential are shown by (blue) circles, and those without the bump by (red) crosses. Left panel: the strength of the first-order EWPT  $\xi$ , defined in Eq. (15), vs Higgs cubic self-coupling. Right panel: Higgs cubic self-coupling vs Higgs mass for points exhibiting a strong first-order EWPT,  $\xi > 1$ . In both plots, the Higgs self-coupling is normalized to the tree-level SM expectation for the same  $m_h$ .

This approximation greatly speeds up the numerical analysis. We performed a partial scan of the parameter space of the model, setting  $a_2 = 0$  and scanning  $a_1 = -150 \dots -50$  GeV,  $b_3 = -150 \dots -50$  GeV,  $\lambda = 0.15 \dots 0.25$ ,  $x = 150 \dots 250$  GeV, and  $b_4 = 0.5$ . This parameter region includes a large set of points with strong first-order EWPT, and lies roughly within the range consistent with precision electroweak constraints<sup>4</sup> determined in [25]. The results of this scan are illustrated in Fig. 5. The models with strong first-order EWPT predict a suppression of the Higgs cubic self-coupling relative to the SM value, by a factor of 2 or more. The sign of the effect, however, is not unique in this model; for example, we found points with  $a_2 \neq 0$  which predict a strong first-order EWPT and an enhanced Higgs self-coupling. The important point is that large, order-one deviations in  $\lambda_3$  from the SM are typical. This is not surprising, since both of these deviations and the possibility of strong first-order EWPT are due to the same new tree-level interactions.

The correlation between the size of this effect and the strength of the EWPT is less clear than in the examples of Secs. II and III. This is simply due to a large number of parameters that affect  $\lambda_3$ , but have only a marginal effect on  $\xi$ . If those parameters are fixed, and, for example, only the Higgs-singlet mixing parameter  $a_1$  is varied, a clear correlation between  $\lambda_3$  and  $\xi$  emerges, as seen in Fig. 6. (In this figure we fixed  $b_3 = -80$  GeV,  $\lambda = 0.20$ ,  $x = 150$  GeV,  $b_4 = 0.5$ ,  $a_2 = 0$ , and scanned  $a_1 = -130 \dots -105$  GeV.)

<sup>4</sup>Note, however, that other new weak-scale states can contribute to precision electroweak observables and modify the fits, without changing the dynamics of the EWPT. A SM-like Higgs in the 300–800 GeV mass range is allowed if new physics produces a positive contribution to the  $T$  parameter. This is the case, for example, in the LHT model [27].

Unlike the models of Secs. II and III, where the non-standard Higgs cubic coupling might provide the first experimental hint of the existence of extra singlet scalars at the weak scale, the model studied here will provide a variety of deviations in the Higgs production cross section and branching ratios from the SM due to the singlet admixture [25]. Many such deviations will probably be observed before the Higgs self-coupling measurement is available. Nevertheless, it is interesting that the general

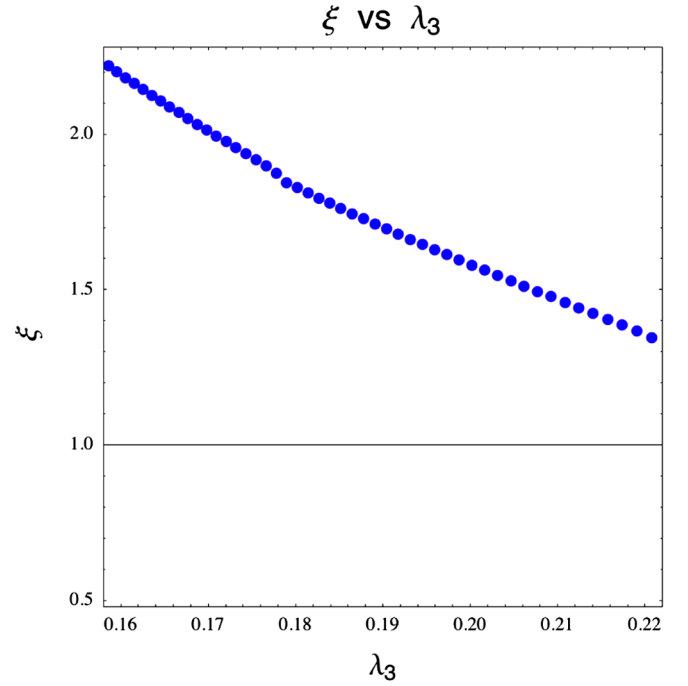


FIG. 6 (color online). The strength of the first-order EWPT  $\xi$  vs Higgs cubic self-coupling, in the model of Eq. (24). Only the mixing parameter,  $a_1$ , is varied. The Higgs self-coupling is normalized to the one-loop SM expectation for the same  $m_h$ .

pattern of large deviations in  $\lambda_3$  in all models exhibiting a strong first-order EWPT persists in this class of models.

## V. CONCLUSIONS

In this paper, we investigated the link between the dynamics of the EWPT and the deviation of the cubic Higgs boson self-coupling in extensions of the SM. We studied this link in a series of toy models. Our toy models implement three mechanisms by which the weak-scale new physics could turn the second-order (or crossover) adiabatic transition predicted in the pure SM into a first-order transition. In the first set of models, the dynamics is determined by large quantum corrections to the Higgs potential, both zero- and finite-temperature, from loops of new particles (possibly, but not necessarily, gauge singlets) with strong coupling to the Higgs. In the second model, the first-order transition is due to the presence of a nonrenormalizable operator in the Higgs potential. In the third model, the crucial new feature is the tree-level mixing between the Higgs and an extra scalar singlet. In all cases, we found that models that exhibit a strong first-order EWPT predict large deviations of the Higgs cubic coupling from the standard model value. Order-one deviations are typical. The models of the first and second classes typically predict an enhancement in the Higgs cubic coupling, while in the models of the third class both signs are equally likely. The only cases where the cubic coupling does *not* deviate significantly from the SM prediction are due to accidental cancellations among unrelated contributions to this coupling. Thus, we conclude that a measurement of the Higgs cubic coupling consistent with the SM prediction would strongly disfavor (although not completely rule out) a first-order electroweak phase transition. A discovery of a substantial deviation of this coupling from the SM would keep the possibility of a first-order transition open, but would not conclusively prove it, as discussed at the end of Sec. II A.

While a measurement of the Higgs cubic coupling is very difficult at the LHC, a 20%-level measurement appears to be within the reach of the proposed luminosity or energy upgrades of the LHC, as well as the ILC. Based on the analysis, we conclude that such a measurement could

serve as a sensitive probe of the dynamics of the electroweak phase transition. If no deviation from the SM is observed, it would be very unlikely that the transition is first order. Note that at least some of the sources of the first-order transition are very difficult to exclude by any other means: for example, a gauge-singlet scalar that does not mix with the Higgs at tree level but has a strong quadratic coupling, as in the model of Sec. II A, is essentially impossible to detect directly as long as the decay  $h \rightarrow SS$  is kinematically forbidden. Therefore, even with a large body of knowledge about the BSM particles and their couplings from the LHC and ILC experiments, the question of the order of the phase transition would be very difficult to settle definitively. A measurement of the Higgs cubic coupling would be crucial in addressing this issue.

It is exciting that the next generation of collider experiments will likely contribute to our understanding of cosmology. One example is the possibility that the dark matter particle will be discovered, and its properties measured, at the LHC and the ILC. This connection has attracted much attention in the literature, and has been analyzed both in specific models of new physics [28], and in a model-independent framework [29]. Understanding the dynamics of the electroweak phase transition is another open question in the early universe cosmology where the LHC and ILC experiments will have an important role to play. In this paper, we studied one simple experimentally observable quantity that is tightly correlated with the order of the transition. It is also possible that a combination of mass and coupling measurements could be used to completely reconstruct the Higgs potential, providing a much more detailed picture of the transition. It would be interesting to understand what quantities would need to be measured, and how precise the measurements would need to be.

## ACKNOWLEDGMENTS

We are grateful to Sohag Gandhi, Christophe Grojean, and Geraldine Servant for useful discussions. We are also very grateful to David Rainwater for a communication regarding the prospects for a measurement of  $\lambda_3$  at the LHC. This research is supported by the NSF Grant No. PHY-0355005.

- 
- [1] D. A. Kirzhnits, Pis'ma Zh. Eksp. Teor. Fiz. **15**, 745 (1972) [JETP Lett. **15**, 529 (1972)]; D. A. Kirzhnits and A. D. Linde, Phys. Lett. **42B**, 471 (1972).
  - [2] M. E. Shaposhnikov, Nucl. Phys. **B287**, 757 (1987); **B299**, 797 (1988). For reviews of more recent developments, see A. Riotto and M. Trodden, Annu. Rev. Nucl. Part. Sci. **49**, 35 (1999); M. Dine and A. Kusenko, Rev. Mod. Phys. **76**, S1 (2004).
  - [3] C. Grojean and G. Servant, Phys. Rev. D **75**, 043507 (2007); C. Caprini, R. Durrer, and G. Servant, Phys. Rev. D **77**, 124015 (2008).
  - [4] K. Kajantie, M. Laine, K. Rummukainen, and M. E. Shaposhnikov, Nucl. Phys. **B466**, 189 (1996); Phys. Rev. Lett. **77**, 2887 (1996); Nucl. Phys. **B493**, 413 (1997); M. Gurtler, E. M. Ilgenfritz, and A. Schiller, Phys. Rev. D **56**, 3888 (1997); F. Csikor, Z. Fodor, and J. Heitger, Phys.

- Rev. Lett. **82**, 21 (1999).
- [5] C. Grojean, G. Servant, and J. D. Wells, Phys. Rev. D **71**, 036001 (2005).
  - [6] S. Kanemura, Y. Okada, and E. Senaha, Phys. Lett. B **606**, 361 (2005); *Proceedings of 2005 International Linear Collider Workshop (LCWS 2005), Stanford, California, 2005*, arXiv:hep-ph/0507259, p. 0704; S. W. Ham and S. K. Oh, arXiv:hep-ph/0502116.
  - [7] For reviews, see H. E. Haber and G. L. Kane, Phys. Rep. **117**, 75 (1985); S. P. Martin, arXiv:hep-ph/9709356.
  - [8] For reviews, see M. Schmaltz and D. Tucker-Smith, Annu. Rev. Nucl. Part. Sci. **55**, 229 (2005); M. Perelstein, Prog. Part. Nucl. Phys. **58**, 247 (2007).
  - [9] G. W. Anderson and L. J. Hall, Phys. Rev. D **45**, 2685 (1992).
  - [10] L. Dolan and R. Jackiw, Phys. Rev. D **9**, 3320 (1974); S. Weinberg, Phys. Rev. D **9**, 3357 (1974).
  - [11] M. E. Carrington, Phys. Rev. D **45**, 2933 (1992).
  - [12] E. J. Weinberg and A. Wu, Phys. Rev. D **36**, 2474 (1987).
  - [13] U. Baur, T. Plehn, and D. L. Rainwater, Phys. Rev. Lett. **89**, 151801 (2002).
  - [14] U. Baur, T. Plehn, and D. L. Rainwater, Phys. Rev. D **67**, 033003 (2003).
  - [15] U. Baur, T. Plehn, and D. L. Rainwater, Phys. Rev. D **69**, 053004 (2004).
  - [16] C. Castanier, P. Gay, P. Lutz, and J. Orloff, arXiv:hep-ex/0101028.
  - [17] A. Djouadi, J. Lykken, K. Monig, Y. Okada, M. J. Oreglia, and S. Yamashita, arXiv:0709.1893.
  - [18] S. R. Coleman and E. Weinberg, Phys. Rev. D **7**, 1888 (1973).
  - [19] W. D. Goldberger, B. Grinstein, and W. Skiba, Phys. Rev. Lett. **100**, 111802 (2008).
  - [20] J. R. Espinosa and M. Quiros, Phys. Rev. D **76**, 076004 (2007).
  - [21] S. J. Huber and T. Konstandin, J. Cosmol. Astropart. Phys. **05** (2008) 017.
  - [22] C. Delaunay, C. Grojean, and J. D. Wells, J. High Energy Phys. **04** (2008) 029.
  - [23] G. F. Giudice, C. Grojean, A. Pomarol, and R. Rattazzi, J. High Energy Phys. **06** (2007) 045.
  - [24] See, for example, M. Pietroni, Nucl. Phys. **B402**, 27 (1993); S. J. Huber and M. G. Schmidt, Nucl. Phys. **B606**, 183 (2001); A. Menon, D. E. Morrissey, and C. E. M. Wagner, Phys. Rev. D **70**, 035005 (2004); C. Balazs, M. S. Carena, A. Freitas, and C. E. M. Wagner, J. High Energy Phys. **06** (2007) 066.
  - [25] S. Profumo, M. J. Ramsey-Musolf, and G. Shaughnessy, J. High Energy Phys. **08** (2007) 010.
  - [26] A. Ahriche, Phys. Rev. D **75**, 083522 (2007).
  - [27] J. Hubisz, P. Meade, A. Noble, and M. Perelstein, J. High Energy Phys. **01** (2006) 135.
  - [28] See, for example, E. A. Baltz, M. Battaglia, M. E. Peskin, and T. Wizansky, Phys. Rev. D **74**, 103521 (2006).
  - [29] A. Birkedal, K. Matchev, and M. Perelstein, Phys. Rev. D **70**, 077701 (2004); C. Bartels and J. List, arXiv:0709.2629.